

The Role of Volatiles in the Thermal History of Metamorphic Terranes

by JOHN B. BRADY

Geology Department, Smith College, Northampton, MA 01063

(Received 9 September 1987; revised typescript accepted 25 April 1988)

ABSTRACT

Analytical and numerical solutions to the differential equations for the conduction of heat with heat production or with fluid flow have been used to evaluate the role of volatiles in the thermal history of regional metamorphic terranes. The maximum thermal effect from pervasive, single-pass, regional volatile flow may be predicted from a steady-state solution given by Bredehoeft & Papadopoulos (1965). For fluid velocity v_F (m/s) and connected porosity ϕ , combinations of volatile flux $v_F\phi$ (m^3 of fluid/ m^2s) and transport distance L (m) such that $v_F\phi L$ is greater than 3.6×10^{-7} should produce regional temperature increases due to fluid flow, if the flow persists for 10^5 – 10^6 a (depending on the transport distance L). The absolute value of the temperature increase due to volatile flow will be greater in regions with higher ambient geothermal gradients. For $L = 20$ km, a volatile flux of 1.8×10^{-11} (m^3 of fluid/ m^2s) or greater is required to achieve a temperature effect. Few geologic processes release volatiles at this rate for extended periods of time, so regional thermal effects from the single-pass, pervasive flow of volatiles are unlikely. A new analytical solution for the steady state temperature distribution between idealized parallel channels of fluid flow is presented along with the results of two-dimensional numerical models of channelized fluid flow. Both approaches show that little temperature increase is expected near channels of fluid flow relative to the rocks between the channels, unless the channels exceed 100 m in width or unless the fluid fluxes are very large and transient. A possible thermal effect of volatile flow in metamorphic terranes is the production of metamorphic hot spots due to focusing of volatiles into widely spaced channels or conduits exceeding 1 km in width. Given a sufficient fluid flux (exceeding 10^{-10} m^3 of fluid/ m^2s), thermal gradients of over 100 K from center to edge may be produced in such channels during relatively short time intervals (10^5 – 10^6 a).

NOMENCLATURE

A	a constant
A_0	'heat production' due to fluid flow ($\text{J}/\text{m}^3\text{s}$)
B	a constant defined in equation (4)
C	a constant
$C_{P,F}$	isobaric specific heat of the fluid ($\text{J}/\text{kg}\cdot\text{K}$)
$C_{P,R}$	isobaric specific heat of the (wet) rock ($\text{J}/\text{kg}\cdot\text{K}$)
$C_{P,S}$	isobaric specific heat of the dry rock ($\text{J}/\text{kg}\cdot\text{K}$)
E_x	net energy gain ($\text{J}/\text{m}^3\text{s}$)
J_z^{fixed}	heat flux in the z direction with respect to a fixed reference frame ($\text{J}/\text{m}^2\text{s}$)
J_z^{IRF}	heat flux in the z direction with respect to a moving reference frame ($\text{J}/\text{m}^2\text{s}$)
k_1	a constant
K_F	thermal conductivity of a fluid (J/mKs)
K_R	thermal conductivity of a rock (including pore fluid) (J/mKs)
L	thickness of the model slab of equation (1) (m)
P	pressure (Pa)
q_1	a constant heat flux given in equation (10) ($\text{J}/\text{m}^2\text{s}$)
q_2	a constant heat flux given in equation (12) ($\text{J}/\text{m}^2\text{s}$)
Q	a constant heat flux ($\text{J}/\text{m}^2\text{s}$) used in equations (7) and (8)
R_F	radius of a cylindrical fluid conduit (m)

t	time (s) or (a)
t_c	a length of time defined by equation (13) (s) or (a)
T	temperature (K)
T_0	temperature at $Z=0$ or $x=0$ (K)
T_L	temperature at $Z=-1$ or $x=-L$ (K)
T'	normalized temperature $(T-T_0)/(T_L-T_0)$
v_F	fluid velocity (actual) (m/s)
W_F	half-width of a channel of fluid flow (m)
W_R	half-width of the region between fluid flow channels (m)
z	depth (m)
Z	normalized distance ($\equiv z/L$)
γ	Euler's constant ($\equiv 0.57722$. . .) in equation (12)
γ	dimensionless parameter ($\equiv 4kt/W_F^2$) in equations (16) and (17)
ϕ	porosity
ϕ_c	porosity of a channel of fluid flow
κ	thermal diffusivity (m^2/s)
ρ_F	density of the fluid (kg/m^3)
ρ_R	density of the rock (kg/m^3)
ρ_S	density of the dry rock (kg/m^3)

INTRODUCTION

Scientific, technological, and conceptual advances over the last few decades have brought metamorphic petrology to the point where the pressure-temperature-time (P - T - t) history of metamorphic terranes can be discussed quantitatively. Thermal models abound in the recent literature for orogenies both hypothetical (e.g., Shimazu, 1961; Richardson, 1970; Oxburgh & Turcotte, 1971; Wells, 1980; Fowler & Nisbet, 1982; Nisbet, & Fowler, 1982; England & Thompson, 1984; Davy & Gillet, 1986) and real (e.g., Clark & Jäger, 1969; Oxburgh & Turcotte, 1974; Richardson & Powell, 1976; England, 1978; Rubie, 1984). Petrologists are beginning to interpret their field and laboratory data in terms of these models (e.g., Crawford & Mark, 1982; Hollister, 1982; Royden & Hodges, 1984; Chamberlain & England, 1985). Each model is necessarily built upon an array of assumptions that reduce the mathematical complexity to manageable proportions, even though some of the assumptions might not be warranted in cases of interest. In particular, except for hydrothermal convection in the vicinity of shallow intrusives, the transfer of heat by the flow of water and other volatiles is typically not included in the analysis.

England & Thompson (1984) neglected fluid flow in their crustal scale models because they felt that thermal convection is unlikely to occur in the deep crust where porosity and permeability are low, and that the fluid flux due to metamorphic devolatilization reactions would be too small to have a significant effect. Etheridge *et al.* (1983), however, argue that convection is possible for the high fluid pressures and consequent increased permeability that may occur during metamorphism. Certainly, *forced* flow of volatiles can occur in rocks where permeabilities are much too low to permit thermal convection. Indeed, one of the most significant features of the metamorphism of sedimentary rocks is the loss of water that occurs. Pore water is lost due to compaction and structural water is lost as a result of dehydration reactions. Because of the high porosity and water content of young sediments and the significant compaction that occurs during burial, thermal models of sedimentary basins commonly consider forced fluid flow (e.g., Skempton, 1970; Sharp & Domenico, 1976; Stegena, 1982). Even highly compacted shale, however, still has 2-3 wt.% water to lose *en route* to becoming a gneiss. Does the loss of this water and other volatiles lead to a transport of heat that significantly affects the history of a metamorphic terrane on a regional or local scale?

A positive answer to this question could open a new range of possibilities for metamorphic P - T - t paths. For example, England & Thompson (1984) and others have clearly shown that crustal thickening coupled with erosion can lead to heating and metamorphism of the crust. However, only extreme choices of their variable parameters produced the high T , low P conditions observed in Buchan style metamorphic terranes, supporting the view that magmatic activity or special circumstances are required for high T , low P metamorphism (see Jaupart & Provost, 1985). Can forced volatile flow lead to regional, non-magmatic high T , low P metamorphism as suggested by Hoisch (1987)? If the flow of metamorphic dehydration water is channelized as suggested by Norris & Henley (1976), Walther & Orville (1982), Ferry (1987), Chamberlain & Rumble (1988) and others, what thermal effects might be expected near the channels? Might other sources of fluid, such as the dehydration of subducted crust, the rapid dehydration of autochthonous sediments following thrusting, or mantle degassing, lead to significant metamorphic effects as proposed by Schuiling & Kreulen (1979) and others? These and related questions concerning heat and water are examined in the paragraphs that follow.

PERVASIVE VOLATILE FLOW

How much volatile flow is needed to affect temperatures on a crustal scale? An answer to this question can be found in a steady-state solution to the one-dimensional heat conduction equation with fluid flow added. If the crust or a portion of the crust were to experience a steady flow of volatiles from depth toward the surface, temperatures would be elevated relative to a conduction geotherm. As temperatures rise, however, temperature gradients near the surface and conductive heat loss to the surface must increase. If the volatile flow continues long enough, temperatures will rise until a steady state is achieved in which the heat added by conduction and fluid flow from below is exactly balanced by heat loss to the surface (by conduction and fluid flow). Therefore, a steady-state solution to the heat conduction equation modified for volatile flow will provide the *maximum* expected increase of temperature due to volatile flow.

Steady-state model

Consider an 'infinite slab' (an idealized crust) of uniform, permeable rock bounded above and below by parallel planar surfaces (at $z=0$ and $z=-L$). Let a fluid flow upward through the connected porosity (ϕ) of the slab at a constant velocity v_F (m/s), low enough to permit the flowing fluid to maintain thermal equilibrium with the adjacent rock. Assume that the rock (including pore fluid) has a constant effective thermal conductivity K_R (J/msK) and a constant heat capacity per unit volume (J/m³K) given by $[(1-\phi)\rho_S C_{P,S} + \phi\rho_F C_{P,F}]$, where ρ_S and ρ_F (kg/m³) are the densities and $C_{P,S}$ and $C_{P,F}$ (J/kg·K) are the isobaric specific heats of the dry rock and pore fluid, respectively. The change of temperature with time at any point within the slab is described by

$$\left(\frac{\partial T}{\partial t}\right)[(1-\phi)\rho_S C_{P,S} + \phi\rho_F C_{P,F}] = K_R \left(\frac{\partial^2 T}{\partial z^2}\right) - v_F \phi \rho_F C_{P,F} \left(\frac{\partial T}{\partial z}\right). \quad (1)$$

T (K) is temperature, t (s) is time, z (m) is distance measured perpendicular to the parallel surfaces. Equation (1) is an expression of the law of conservation of energy in the absence of heat sources or sinks (e.g., Donaldson, 1962; Stallman, 1963). It should be noted that the velocity v_F used here is the actual or 'seepage' velocity (Fetter, 1980, p. 116), whereas the

velocity used by Stallman (1963) is the fluid flux (per unit area per unit time) or Darcy velocity ($v_F \phi$).

Substituting $Z \equiv z/L$ to make distance dimensionless, equation (1) becomes

$$\left(\frac{\partial T}{\partial t}\right) [(1-\phi)\rho_S C_{P,S} + \phi\rho_F C_{P,F}] = \frac{K_R}{L^2} \left(\frac{\partial^2 T}{\partial Z^2}\right) - \frac{v_F \phi \rho_F C_{P,F}}{L} \left(\frac{\partial T}{\partial Z}\right). \quad (2)$$

In the steady state ($\partial T/\partial t = 0$), equation (2) reduces to the simple form

$$\left(\frac{\partial^2 T}{\partial Z^2}\right) = B \left(\frac{\partial T}{\partial Z}\right) \quad (3)$$

with B given by

$$B = \frac{v_F \phi L \rho_F C_{P,F}}{K_R} \quad (4)$$

and with solutions of the form

$$T = A \cdot \exp(B \cdot Z) + C. \quad (5)$$

where A and C are constants. Choosing constant temperature boundary conditions ($T = T_0$ at $Z = 0$, $T = T_L$ at $Z = -1$), and defining a dimensionless temperature $T' \equiv (T - T_0)/(T_L - T_0)$, the solution (5) becomes

$$T' = \frac{1 - \exp(BZ)}{1 - \exp(-B)} \quad (6)$$

(Bredehoeft & Papadopoulos, 1965). A graphical presentation of (6) is given in Fig. 1 for various values of B , which is similar to a thermal Peclet number.* Figure 1 may be viewed as showing the maximum effect of upward volatile flow on a simple linear (no heat production) geotherm for specific volatile fluxes. For $B = 0.5$, the thermal effects of fluid flow are noticeable with maximum temperature increases of about 30 K for a 20 km slab and an initial gradient of 30 K/km. For $B = 2.0$, maximum temperature increases of over 140 K are expected for the same initial conditions. Clearly, values of B as large as 2.0 can have a dramatic effect on the steady state fluid flow geotherm. Note that equation (6) and Fig. 1 give relative temperatures. Larger absolute temperature increases will occur in regions that have larger initial gradients.

One might assume that a constant conductive flux of heat into the base of the slab would more closely approximate many geologic situations than a constant basal temperature. In this case, the lower boundary condition is $\partial T/\partial Z = -QL/K$ at $Z = -1$, where Q (J/m^2s) is the constant conductive heat flux from below. The solution (5) and its rearrangement (6) are

* Bickle & McKenzie (1987) present a solution to a slightly simplified version of equation (1) in which they neglect the difference between the heat capacities per unit volume of the fluid ($\rho_F C_{P,F}$) and the rock $[(1-\phi)\rho_S C_{P,S} + \phi\rho_F C_{P,F}]$ (see Table 1). Their solutions are given in terms of a thermal Peclet number, Pe , which is related to B by the expression

$$Pe = B \left[\frac{(1-\phi)\rho_S C_{P,S} + \phi\rho_F C_{P,F}}{\rho_F C_{P,F}} \right].$$

For the case that $B \gg 1$, the solution (6) becomes

$$T' = 1 - \exp(BZ),$$

which is identical to the steady-state result found by Bickle & McKenzie (1987, eq. 20) for the same boundary conditions, if $Pe = B$.

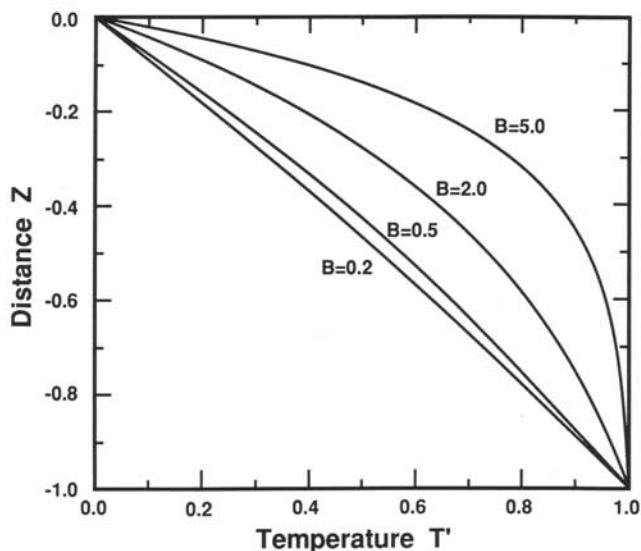


FIG. 1. Normalized temperature $T' \equiv (T - T_0)/(T_L - T_0)$ shown as a function of normalized distance $Z \equiv z/L$ as described by equation (6) for various values of the dimensionless parameter B defined in equation (4). In effect, the curves shown are steady-state geotherms for a model crust with constant volatile flux upward from $Z = -1.0$ to the surface at $Z = 0$. Values of $B \geq 0.5$ lead to a geotherm that differs significantly from the no fluid flow (linear) geotherm.

also correct for the modified boundary conditions, but with constants A and C changed to yield:

$$T = T_0 + [1 - \exp(BZ)] \left[\frac{QL \exp(B)}{BK_R} \right]. \quad (7)$$

Solving for T_L , however,

$$T_L = T_0 + \left(\frac{QL}{BK} \right) [\exp(B) - 1]. \quad (8)$$

yields unrealistically high temperatures for even modest values Q and B . Flowing fluid reduces the temperature gradient required to maintain a constant heat flux from below so that the boundary condition $\partial T/\partial Z = -QL/K$ at $Z = -1$ does not approximate a likely geologic constraint.

Of the parameters in B , the fluid flux (the product of the fluid velocity v_F and the connected porosity ϕ) and the scale length L are most subject to uncertainty or variation. Values of the volumetric heat capacity at constant pressure ($\rho_F C_{P,F}$) for water and carbon dioxide listed in Table 1 show little variation along metamorphic geotherms. Although the volumetric heat capacity of carbon dioxide is only half that of water for the same conditions, metamorphic fluids are typically water rich. Therefore, restricting our attention to the physical conditions of regional metamorphism, a constant value for $\rho_F C_{P,F}$ of 3.5×10^6 (J/m³K) will be used. Thermal conductivity may vary by a factor of two or more, but no simple model is generally applicable. A constant thermal conductivity K_R of 2.5 (J/msK) is assumed throughout this paper (see England & Thompson, 1984, p. 899). For illustrative purposes, consider a scale length L of 20 km to focus on crustal scale processes. Interestingly, doubling or halving this parameter will have the same effect on B as doubling or halving the fluid flux. Using $\rho_F C_{P,F}$,

TABLE 1

Volumetric heat capacity of water at constant pressure ($\rho_F C_{P,F}$) $\times 10^{-6}$ (J/m³K)

T°C	Pressure (kb)							
	1	2	3	4	5	6	7	8
100	4.04	4.05	4.09	4.11	4.14	4.19	4.23	4.26
200	3.84	3.83	3.86	3.91	3.96	3.99	4.04	4.08
300	3.61	3.58	3.64	3.69	3.74	3.81	3.84	3.92
400	3.41	3.36	3.42	3.47	3.53	3.59	3.64	3.71
500	2.91	3.14	3.25	3.28	3.35	3.40	3.49	3.57
600	1.95	2.69	2.91	3.08	3.20	3.30	3.39	3.49
700	1.21	2.11	2.48	2.70	2.85	2.96	3.05	3.13

Data from Helgeson & Kirkham (1974, tables 3 and 34).

Volumetric heat capacity of carbon dioxide at constant pressure ($\rho_F C_{P,F}$) $\times 10^{-6}$ (J/m³K)

T°K	Pressure (kb)				
	1	2.5	5	7.5	10
400	1.33	1.73	1.77	1.80	1.81
500	1.11	1.59	1.74	1.80	1.82
600	0.91	1.24	1.69	1.79	1.85
700	0.77	1.17	1.62	1.77	1.85
800	0.68	1.10	1.53	1.73	1.84
900	0.61	1.03	1.45	1.68	1.82
1000	0.55	0.97	1.26	1.62	1.78

Data from Bottinga & Richet (1981, tables 4 and 10).

K_R , and L as defined above, a fluid flux of $v_F \phi = 1.8 \times 10^{-11}$ (m³ of fluid/m²s) will yield $B = 0.5$. If the porosity ϕ is 0.01, too high perhaps for the deeper crust and too low for shallow rocks, $v_F = 5.6$ (cm/a) for this fluid flux. The same relative effect for a 10 km slab would be produced by a fluid flux of 3.6×10^{-11} (m³ of fluid/m²s). Clearly, volatile flows over 10^{-11} (m³ of fluid/m²s) (velocities over a few centimeters per year for $\phi = 0.01$) may be significant on a crustal scale, if the flow of volatiles continues until a steady state is established.

Time

Although equation (6) gives the magnitude of the maximum thermal effect due to fluid flow as a function of the important variables, it provides no hint of the length of time required to achieve this effect. Can a thermal steady state with volatile flow added to conduction be established within the time span of a metamorphic event? Time may be introduced with the help of some numerical solutions to equation (1) or more elegantly with the analytical solution of Bickle & McKenzie (1987). Their equation (24) gives the time t_c required to achieve approximately 2/3 of the temperature perturbation from a linear gradient in response to fluid flow as

$$t_c \approx \frac{L^2 [(1-\phi)\rho_S C_{P,S} + \phi\rho_F C_{P,F}]}{K_R \left(\pi^2 + \frac{B^2}{4} \right)} \quad (9)$$

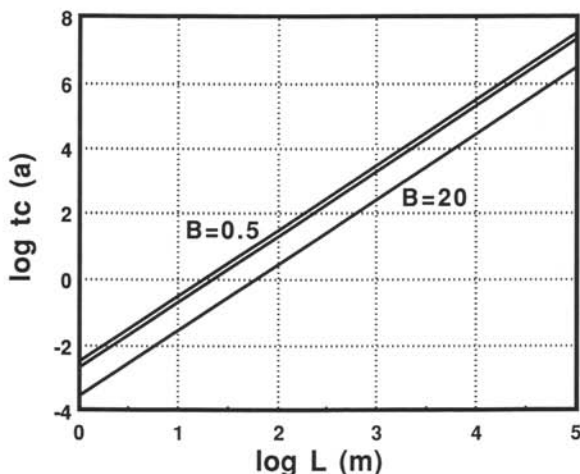


FIG. 2. The time t_c required to achieve the majority of the temperature adjustment expected in a model crust perturbed by upward fluid flow is shown on a logarithmic scale as a function of the thickness L of the crustal slab involved, also on a logarithmic scale, for various values (0.5, 2.0, 20.0) of the parameter B defined in equation (4). The lines are calculated from equation (24) of Bickle & McKenzie (1987). Significant temperature changes may be produced in 1 Ma or less by crustal-scale fluid flow.

The time required to reach the steady state is a function of the square of the thickness of the slab. The variation of t_c with slab thickness and B is shown in Fig. 2. It appears that the small temperature effects due to fluid flow may be achieved quite rapidly in thin bounded slabs.

When numerical methods are used, equation (1) may be tackled in a way that includes more of the complexity of the earth's crust. Figure 3 shows the results, in 0.4 Ma intervals, of adding volatile flow to the top 20 km of a hypothetical crust with a 'normal' conductive geotherm based on a detailed numerical model that includes heat production, a variable thermal conductivity and heat capacity, and a constant conductive heat flux from below. For clarity a fluid flux of 1.6×10^{-10} (m^3 of fluid/ m^2s) and values of K_R and $(\rho_F C_{P,F})$ to give $B \approx 4.7$ are used. Evidently, significant regional thermal excursions can be caused by volatile fluxes lasting less than 1 Ma.

Permeability

If metamorphic rocks have low permeabilities, is it reasonable to consider fluid flows of even 10^{-11} (m^3 of fluid/ m^2s)? Brace (1980, 1984) lists laboratory and *in situ* measurements of permeabilities for crystalline rocks in the range 10^{-21} – 10^{-13} m^2 . Whether the larger permeabilities can persist in a rock undergoing metamorphism is unknown. However, Brace *et al.* (1968) showed that the permeability of Westerly granite increased with decreasing effective pressure ($P_{\text{Total}} - P_{\text{Fluid}}$). Brace *et al.* attributed this effect to microcracks that close as effective pressure rises. The experiments of Brace *et al.* and similar measurements by Pratt *et al.* (1977) indicate that high fluid pressures (low effective pressures) should lead to the maximum permeabilities for a given set of conditions. High fluid pressures are believed to develop during metamorphism, enhancing permeability, when devolatilization reactions are occurring (Fyfe *et al.*, 1978, Chap 10; Etheridge *et al.*, 1983). For the calculation that follows, a permeability of 10^{-18} m^2 will be used, well below what Etheridge *et al.* (1983) consider possible (10^{-18} – 10^{-15} m^2), but well above the values measured by Brace *et al.* (1968) for granite at high effective pressures (10^{-21} m^2).

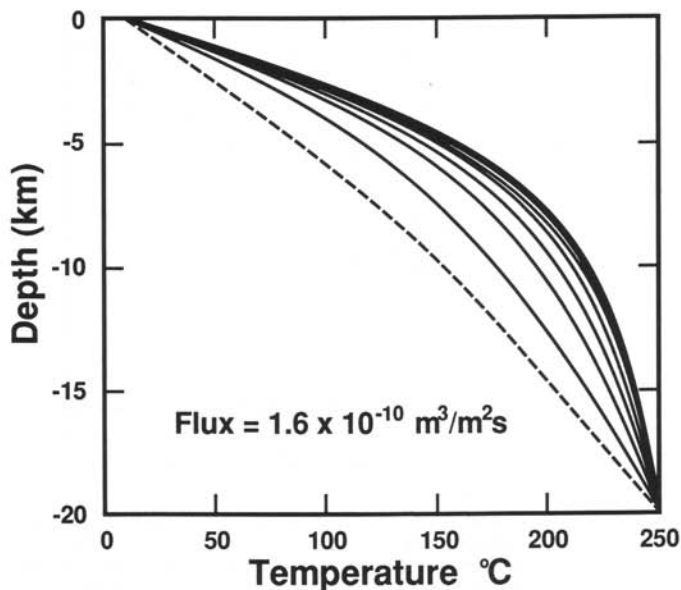


FIG. 3. Temperature shown as a function of depth for 0.4 Ma intervals in an approach to the steady state computed by a finite difference approximation to equation (1) for a model crustal slab 20 km thick. A pervasive fluid flux of $1.6 \times 10^{-10} \text{ m}^3/\text{m}^2\text{s}$ was initiated at $t=0$ when the steady state geotherm was the dashed curve. Model heat production and conductive heat flux from below that produced the initial geotherm and heat flow ($49 \text{ mW}/\text{m}^2$) were continued during the numerical experiment ($B \approx 4.7$). Results of this numerical model are in good agreement with predictions of the analytical solution for the less complex model of Bickle & McKenzie (1987) shown in Fig. 2. Significant temperature changes are observed in less than 1 Ma and a steady state is nearly achieved within 2 Ma.

The maximum pressure gradient normally available to drive vertical fluid flow on a crustal scale is the difference between the lithostatic gradient and the hydrostatic gradient (see Walther & Orville, 1982). Using this differential pressure gradient ($1.9 \times 10^4 \text{ Pa}/\text{m}$ for a crustal density of 2.8 and a fluid density of 0.9), using a fluid viscosity of $1.5 \times 10^{-4} \text{ (kg/ms)}$ (see Walton (1960), Ahrens & Schubert (1975)), and using a permeability of 10^{-18} m^2 , Darcy's Law for fluid flow in a porous medium (Hubbert, 1940) predicts a flux of $1.3 \times 10^{-10} \text{ (m}^3 \text{ of fluid}/\text{m}^2\text{s)}$. A flux of this magnitude through a rock with a flow porosity of 0.01 would require an average fluid flow velocity of 60 (cm/a). Based on these estimates, it appears to be physically possible to have fluid fluxes large enough to cause thermal effects, even in low-permeability metamorphic rocks.

Although a permeability of 10^{-18} m^2 may be too high for many metamorphic rocks, it may be too low for metamorphic rocks fractured by volatile release. If fracturing occurs in response to rising fluid pressure or tectonic events as suggested by Norris & Henley (1976), Fyfe *et al.* (1978), and Walther & Orville (1982), fluid flow may be concentrated along fractures and enhanced. The *thermal* consequences of flow along fractures are similar to the thermal consequences of percolating flow, unless the fractures are widely spaced (see below).

Flux and volume of volatiles released during regional metamorphism

Maintaining a volatile flux of $1.8 \times 10^{-11} \text{ (m}^3 \text{ of fluid}/\text{m}^2\text{s)}$ requires $570 \text{ (m}^3 \text{ of fluid}/\text{m}^2)$ in 1 Ma. Clearly, large volumes of volatiles must be supplied rapidly to maintain the flow rates necessary to cause a crustal scale thermal effect from volatile flow. Walther & Orville (1982)

calculate a *maximum* volatile flux from the regional metamorphism of an average pelite of about 300 (m³ of fluid/m²Ma). Yardley (1986) suggests a *maximum* volatile flux of 420 (m³ of fluid/m²Ma) for regional metamorphism. Based on these estimates, a volatile flux from metamorphic reactions of the magnitude necessary to produce a regional thermal effect appears to demand the special circumstance of rapid heating.

The devolatilization of an average pelite during progressive metamorphism will yield about 5 wt.% fluid with a volume at 500°C and 5 kb of about 12% of the volume of the rock metamorphosed (Walther & Orville, 1982). Therefore, to supply the fluid for a fluid flux of 1.8×10^{-11} (m³ of fluid/m²s) ($B=0.5$) for 1 Ma, the complete dehydration of a 4.7 km thick pile of pelite in one Ma (isograd velocities of 4.7 mm/a) would be needed. Actual rates of metamorphism are believed to be an order of magnitude lower (isograd velocities ≤ 1 mm/a, Brady, 1982; Walther & Orville, 1982; Peacock, 1986). Metamorphism of siliceous dolomites can yield a proportionally much larger volume of fluid than the metamorphism of pelites, as much as 50% of the volume of the rock metamorphosed (Rumble *et al.*, 1982), but siliceous dolomites rarely form a significant fraction of the crust. Metamorphism on a crustal scale is required to supply fluids at the rate of 10^{-11} (m³ of fluid/m²s) for even a few million years, whereas crustal scale metamorphism is likely to require tens of millions of years (e.g., England & Thompson, 1984). Rates of metamorphism are not significantly increased by including the forced convection of evolved fluids. Results of numerical crustal heating experiments in which the advection of evolved metamorphic fluids is included are virtually indistinguishable from conduction only experiments (Brady, 1982). In sum, volatiles produced by metamorphic reactions during most crustal thickening events are not supplied at a rate sufficient to noticeably affect the crustal thermal regime.

LOOKING FOR LARGE FLUID FLUXES

Convection

What tectonic environments might lead to fluid fluxes on the order of 500 m³ of fluid/m²Ma? Convective fluid flow in the neighborhood of shallow (<6 km) intrusives may involve fluxes this large and can have a major thermal effect on both the cooling intrusive and on the surrounding rocks (e.g., Taylor, 1971; Cathles, 1977; Norton & Knight, 1977; Criss & Taylor, 1987). Based on their models, Norton & Knight (1977) compute fluid fluxes that locally exceed 10⁵ m³ of fluid/m²Ma. Similar fluid convection may occur in the vicinity of the deeper intrusives that are commonly found in metamorphic terranes, although estimates of permeability for metamorphic rocks argue against convection (England & Thompson, 1984). Etheridge *et al.* (1983), believing that relatively high permeabilities result from high fluid pressures, suggest that convective circulation, with detailed fluid pathways determined by local structure, can occur during regional metamorphism. Wood & Walther (1986), however, argue that high fluid pressures (greater than hydrostatic) should preclude convection and permit only 'single-pass flow'. The oxygen isotopic data of Wickham & Taylor (1985) for a regional metamorphic terrane in the Pyrenees support the idea of pervasive infiltration and perhaps circulation of a seawater-rich fluid during heating of pelitic metasediments at depths of 6–12 km. Ferry (1986*a, b*) argues that the high (1–5:1) fluid to rock ratios calculated for many metamorphic terranes require a multi-pass (convection) model of fluid flow at depths greater than 10 km. Wood & Walther (1986) give reasons why the calculated fluid to rock ratios might not require multi-pass flow. Clearly, there is no agreement on the possibility of thermal convection of volatiles in the deep crust. The *thermal* effects of convective circulation (the multi-pass model), if it occurs, could be dramatic. Thermal convection requires a different analysis from that presented here for

forced fluid flow, and is not considered further. The conclusions of this paper are based on the assumption of single-pass volatile flow.

Magmatic devolatilization

Although it is not clear whether convective circulation can occur in the vicinity of deep intrusives, deep intrusives can lead to forced fluid flow due to magmatic devolatilization during crystallization. Ferry (1980, 1983) argues on the basis of mineral compositions and modes of metacarbonate rocks that fluid flow during metamorphism increased in the vicinity of two quartz monzonite stocks, possibly recording the loss of fluid from the crystallizing stocks. Magmas can contain several weight per cent of H_2O and CO_2 that may separate into a fluid phase during crystallization. Even so, to have a regional temperature effect from the release of these volatiles, a large magma body such as a batholith would be required. For example, the region overlying an extensive granodiorite intrusion 10 km thick might receive a total flux of 8.4×10^5 (kg water/m²) (730 m³ water/m² at 500°C and 5 kb) from the approximately 3 wt. % water in the granodiorite (Burnham, 1979). This water may be released gradually over the several million years that it may take the intrusion to solidify (Jaeger, 1964) or in pulses as fluid pressure rises during crystallization (Burnham, 1979). Enough water is available in the magma to have a short-lived regional thermal effect, but only if the volatiles are released in 1 Ma or less. A release of volatiles that is focused into broad zones of fluid flow may leave a record in the conduit host rocks (see below). Devolatilization during contact metamorphism of country rocks may produce a small volume of fluid rapidly. Simple calculations suggest that the thermal effects of the movement of this fluid should be small and will not normally be important.

Subduction zone devolatilization

An extensive literature exists on the thermal structure of subduction zones (e.g., McKenzie, 1969; Hasebe *et al.*, 1970; Oxburgh & Turcotte, 1970, 1976; Toksöz *et al.*, 1971; Griggs, 1972; Anderson *et al.*, 1978, 1980; Sydora *et al.*, 1978; Honda & Uyeda, 1983; Wang & Shi, 1984; Honda, 1985). A number of these authors have proposed thermal, chemical, and petrologic effects that may result from the fluid released by compaction and diagenesis in the accretionary wedge and by devolatilization reactions in the subducted oceanic crust. Davis *et al.* (1986) and Reck (1987) call upon upward fluid flow to explain higher than expected heat flow in accretionary prisms in Barbados and northeast Japan, respectively. Reck's (1987) numerical models satisfy observed temperature data (Burch & Langseth, 1981) if upward water fluxes of 10^{-10} (m³ of fluid/m²s) are present. However, upon consideration of the water content of prism sediments, Reck concludes that sufficient fluid fluxes are only possible if the fluid flow is focused into narrow zones (e.g., Cloos, 1984).

Oceanic crust may be hydrated by a number of processes from ridge to subduction zone and some uncertainty exists regarding the actual volatile content of the oceanic crust as it is heated during subduction (Anderson *et al.*, 1976). Release of volatiles is believed to occur in the depth interval 80–125 km (Anderson *et al.*, 1978; Delany & Helgeson, 1978). Flow paths and sinks for these volatiles are the subject of much speculation and few data. It is likely that most of the volatiles are consumed by melting reactions in overlying dry mantle or crustal rocks (e.g., Anderson *et al.*, 1980) and, therefore, participate only indirectly in the metamorphism of upper crustal rocks. Nevertheless, were subducted volatiles able to reach upper crustal regions directly, back up the subduction zone or along other unspecified fluid conduits, a thermal effect might be present (see Hoisch, 1987; Peacock, 1987b). The cardinal

aspect of subduction processes is the comparatively inexhaustible supply of fluid. The major question mark is whether any of these fluids can reach the middle or upper crust without being consumed in melting reactions.

Dehydration of the hypothetical oceanic crustal metamorphic mineral assemblage of Anderson *et al.* (1976, 1978), consisting of 25% chlorite, 25% amphibole, 20% serpentine, 5% talc, and 25% anhydrous minerals, would yield about 178 kg water/m³. Anderson *et al.* (1978) model the dehydration as occurring beneath a 50 km zone parallel to the trench. Assuming a 5 km thick hydrated oceanic crust and a convergence rate of 5 cm/a, water would be released at the rate of 8.9×10^5 (kg/m²Ma) over the 50 km interval. At 500°C and 5 kb, this water flux would be about 2.5×10^{-11} (m³ of fluid/m²s) (= 775 m³ of fluid/m²Ma). Although the oceanic crust may contain less than the approximately 6 wt. % water specified in the above model mineral assemblage, higher convergence rates, subducted sediments, and/or a thicker crust might compensate in individual cases. Peacock (1987*b*) considers this particular problem in more detail. He uses a more conservative estimate of the volatile content of subducted oceanic crust (2 wt. %) and releases these volatiles over a 150 km zone to conclude that the effects of pervasive fluid flow are minimal. Peacock suggests that channelized flow of these fluids in the subduction shear zone may provide a greater localized thermal effect than pervasive flow.

Crustal thickening and thinning

If the rate of metamorphism is tectonically accelerated, significant fluxes of evolved fluids may occur. In particular, heating due to large scale thrusting (e.g., England & Thompson, 1984) or crustal thinning (McKenzie, 1978), may lead to rapid devolatilization and significant fluid fluxes. Emplacement of thrust slices will cause the underlying rocks to be heated, rapidly at first, as the geotherm responds to a thickened crust. If the underlying rocks are sediments or partially dehydrated metasediments, volatiles will be released that may flow through the overlying thrust slice or perhaps upward along the thrust fault zone. Initially, evolved fluids may accelerate cooling and fuel retrograde reactions in the warmer overlying rocks. However, unless the fluid flow is focused, the rate of volatile production is generally not sufficient to change the geotherm from that expected in the absence of fluid flow. This can be demonstrated from numerical experiments analogous to those of England & Thompson (1984) and others, but with volatile production from metamorphic reactions and consequent upward fluid flow added (Brady, 1982). However, a look at the possible volatile production rates based on England & Thompson's (1984) results will provide a more simple proof.

Consider a crust thickened by thrusting with thermal parameters and tectonic chronology corresponding to those of fig. 3e of England & Thompson (1984). Very roughly, 25 km of the lower plate is heated from below 400°C to over 600°C during the first 20 Ma following thrusting. Assuming that the full 25 km contains 5 wt. % volatiles (Wather & Orville's (1982) estimate for the average 'fertile' pelite) and that all of the volatiles are released over the 20 Ma period, a flux of about 180 m³ of fluid/m²Ma would be produced ($B=0.28$ because of the 35 km scale length). Recognizing that these parameter choices have maximized the calculated flow and that features such as multiple, rather than single, thrust slices (Davy & Gillet, 1986) will reduce the rate at which volatiles are released, the thermal impotence of this flow is evident. Focusing the flow of these fluids through broad channels in the upper plate, however, might cause significant local effects (see below).

Metamorphism in response to crustal thinning (e.g., McKenzie, 1978, 1981; Royden & Keen, 1980; Wickham & Oxburgh, 1985; Sandiford & Powell, 1986) may be relatively rapid,

increasing the rate of volatile release over that expected for zones of crustal thickening. The effect of an increased volatile flux, however, is countered by a decreased scale length L as the crust is thinned, so that pervasive single-pass fluid flow is not likely to be important. Interestingly, an extensional environment may facilitate deep circulation of fluids (Wickham & Oxburgh, 1985; Wickham & Taylor, 1985) with possible significant thermal effects.

Mantle devolatilization

Schuilung & Kreulen (1979) postulate that the metamorphic thermal dome at Naxos, Greece may have been caused by a large influx of CO₂-rich fluid of deep seated origin. A large number of workers have suggested that an influx of CO₂-rich fluids may have had an important role in the genesis of granulites, but this suggestion remains a topic of controversy (see Hansen *et al.*, 1984; Bhattacharya & Sen, 1986; Crawford & Hollister, 1986; Newton, 1986). If it can be demonstrated that large volumes CO₂-rich fluids escape from the mantle, the possible thermal consequences are significant and can be estimated using the equations presented here. Spera (1981) estimates a minimum, long-term average rate of volatile outgassing from the mantle by summing the mass of volatiles in the atmosphere, hydrosphere, and sedimentary rocks and dividing by all of geologic time. His result of 4.4×10^{11} (kg/a), averaged over the surface of the earth, is about 2×10^{-14} (m³ of fluid/m²s). Although the large scale length L that would apply to mantle outgassing through continental crust would enhance the thermal effect, considerable focusing is needed for this long-term average flux to have a noticeable effect on crustal temperatures. If, however, most of these volatiles were released early in the earth's history, their flow may have had a major role in determining the geotherm in the early crust.

CHANNELIZED FLUID FLOW

It has been suggested by many geologists that the escape of metamorphic fluids may be localized along planar or cylindrical channels (e.g., Norris & Henley, 1976; Ferry, 1979; Rumble *et al.*, 1982; Walther & Orville, 1982; Chamberlain & Rumble, 1988) and evidence for specific cases of channelized flow of fluid is mounting (e.g., Beach & Fyfe, 1972; Rye *et al.*, 1976; Rumble & Spear, 1983; Kerrich *et al.*, 1984; Nabelek *et al.*, 1984; Bebout & Carlson, 1986; Ferry, 1987). High permeability flow paths due to features such as fracture systems, fault zones, hydrofracturing, and high permeability formations can have a dramatic effect on the metamorphic hydrology and might also affect the temperature distribution in a metamorphic terrane, depending on the distribution of the channels and the total fluid flux. Volatile sources listed above that cannot fuel a regional thermal effect may become significant if the flow is focused along a few channels. For example, Chamberlain & Rumble (1988) attribute localized occurrences of high temperature minerals in New Hampshire to metamorphic 'hot spots' produced by fluid flow, citing oxygen isotopic evidence for large quantities of fluid.

Two questions are of special interest when considering channelized fluid flow: (1) to what extent can the local temperature be raised in the vicinity of the channels, and (2) how does the regional thermal effect of channelized fluid flow differ from that of the pervasive flow of the same quantity of fluid? To answer these questions it is helpful to examine some additional analytical and numerical solutions to the differential equations of heat transfer.

Constant planar source of heat

Fluid flowing in a channel such as a fracture, shear zone, or permeable rock unit provides a source of heat that may be approximated by a constant thermal flux across the planar boundary of the channel. The magnitude of the constant flux q_1 (J/m^2s) is determined by the flow rate of the fluid, the temperature gradient along the channel, the width of the channel, and the heat capacity of the fluid according to the expression

$$q_1 = W_F v_F \phi_C \rho_F C_{P,F} \left(\frac{\partial T}{\partial z} \right) \quad (10)$$

where W_F is the half width of the channel, ϕ_C is the porosity of the channel, and $(\partial T/\partial z)$ is the temperature gradient along the channel. This expression assumes that temperatures are uniform within the channel along planes perpendicular to the direction of fluid flow and that all the available energy is transferred to the rock as the fluid passes, neglecting the small portion of the energy required to raise the temperature of the channel rocks themselves. The result is therefore limited to relatively narrow channels (see below).

A one-dimensional solution is given by Carslaw & Jaeger (1959, p. 75) for a constant planar source of heat in a semi-infinite solid initially at constant temperature T_0 . Although Carslaw & Jaeger give the full solution, the equation of interest is their (2.9.8), which gives the temperature increase of the solid at the boundary of the channel as follows:

$$T - T_0 = \frac{2q_1}{K_R} \sqrt{\frac{\kappa t}{\pi}} \quad (11)$$

In this expression, κ (m^2/s) is the thermal diffusivity of the rocks and the other terms are as defined previously. $T - T_0$ is shown on a logarithmic scale as a function of the steady flux q_1 in Fig. 4 for times t of 10^5 and 10^7 a, $K_R = 2.5$ (J/mKs), and $\kappa = 10^{-6}$ (m^2/s). Based on this

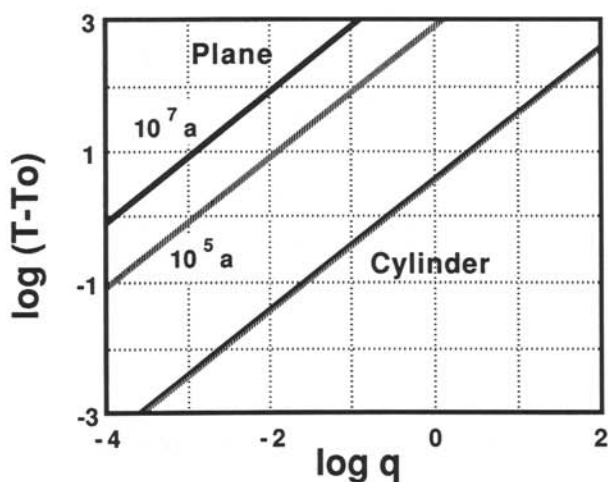


FIG. 4. The increase in temperature ($T - T_0$) at the planar boundary of a semi-finite slab initially at a constant temperature T_0 is shown as a function of a constant heat flux q across the boundary for events lasting 10^5 a and 10^7 a. Equation (11), taken from Carslaw & Jaeger (1959, eq. 2.9.8), was used to compute the figure. According to this model (see text), heat fluxes greater than 10^{-3} J/m^2s are required to produce temperature rises greater than 10 K in 10 Ma. Calculations for a cylindrical model (Carslaw & Jaeger, 1959, eq. 13.5.19) with a radius of 1 m are also shown. Heat fluxes of 10 (J/m^2s) across the boundary of the cylinder are required to produce a 10 K temperature rise in 10 Ma adjacent to the cylinder.

simple model, it appears that q_1 must be greater than 10^{-3} (J/m²s) to have a temperature increase of 10 K near the channel in 1 Ma or less. For a temperature gradient of 30 K/km and $(\rho_F C_{p,F}) = 3.5 \times 10^6$ (J/m³K), a q_1 of 10^{-3} (J/m²s) corresponds to a fluid flux $W_F v_F \rho_C$ per unit length of channel of about 10^{-8} (m³ of fluid/ms) or 300 000 (m³ of fluid/mMa). This fluid flux is about 10^3 greater than the maximum flux estimated for the volatiles evolved during the metamorphism of an average pelite and, therefore, would require focusing of the fluid from pelite underlying a minimum of 1 km² into a 1 km long channel. The exact width of the channel is unimportant as long as the assumption is correct that the heat added to the channel by fluid flow is lost to the adjacent rock at the same rate.

Constant cylindrical source of heat

Fluid flowing in a pipe-like conduit has less influence on its surroundings than fluid flowing in a planar channel at the same flux per unit area of channel. The expression for the temperature increase at the boundary of a cylindrical heat source in a semi-infinite medium, comparable to equation (11), is given by Carslaw & Jaeger (1959, equation 13.5.19) as

$$T - T_0 \cong \frac{q_2 R_F}{2K_R} \left[\ln \left(\frac{4\kappa t}{R_F^2} \right) - \gamma \right]. \quad (12)$$

where q_2 is the heat flux (J/m²s) across the surface of the cylindrical conduit, R_F (m) is the radius of the fluid conduit, γ is Euler's constant (0.57722 . . .), and the other terms are as in (11). $T - T_0$ calculated from equation (12) is shown in Fig. 4 for a conduit with $R_F = 1$ (m) along with the results from equation (11). Because the temperature rises only with the natural logarithm of the time t , the temperature rise for 10^7 a is not much different than that for 10^5 a. For the same rise of temperature, the heat flux q_2 across the surface of a cylindrical conduit must be two to three orders of magnitude higher than the heat flux q_1 across the surface of a planar channel.

Again assuming that all the available energy is transferred to the rock as the fluid passes, q_2 may be expressed in terms of q_1 as follows:

$$q_2 = \frac{R_F v_F \rho_C \rho_F C_{p,F}}{2} \left(\frac{\partial T}{\partial z} \right) = \frac{q_1 R_F}{2W_F}. \quad (13)$$

Using the same parameters as above, a 10 K temperature rise would require a fluid flux $\pi R_F^2 v_F \rho_C$ of about 10^{-5} (m³ of fluid/m²s). This could be accomplished by funnelling the volatiles from pelite underlying a minimum of 1 km² into an open circular conduit with a 1 m² cross-section.

Two-dimensional parallel channel flow

Of the simplifications needed to apply equations (11) and (12), two are particularly troubling. (1) In the earth the problem is at least two-dimensional: fluids will be heating rocks in a geothermal gradient. Heat is conducted toward the surface as well as away from the fluid channel. (2) Fluid pathways may not be isolated so that the interaction of multiple channels may be important. Both of these complications are addressed in a steady state solution derived in the Appendix for the case of constant fluid flow in symmetrically distributed channels of infinite extent (see Fig. 5). Although this geometry is idealized, two-dimensional numerical experiments confirm its utility for estimating the maximum temperature effect of channelized fluid flow (see below). Constant fluid flow advances the isotherms

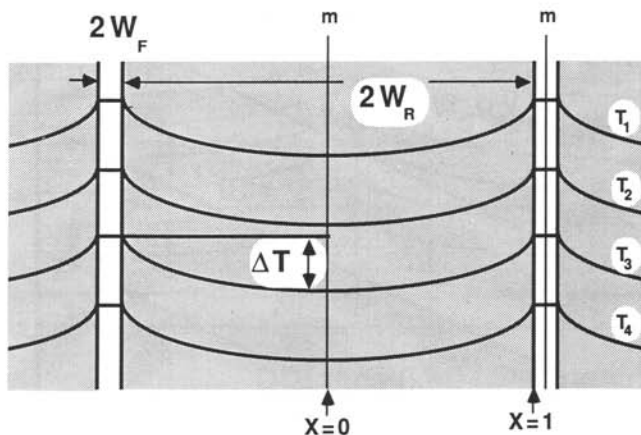


FIG. 5. Isotherms expected between symmetrically positioned, parallel channels of fluid flow in a model, infinite system. Planes of symmetry are indicated by the vertical lines labelled 'm'. If a fluid flows upward in the channels at a constant rate, isotherms will be advanced near the channels until a steady state is achieved. In the steady state, isotherms will move upward at a constant velocity that is proportional to the fluid flux (equation A12). In a reference frame that moves with the isotherms, the isotherm shape is given by equation (A13). ΔT is given by equations (14) and (15).

of a linear temperature gradient such that the isotherms near the channels are bent in the downstream direction (upward in the earth and in Fig. 5). A critical measure of the local thermal effect of channelized fluid flow is the difference in temperature (ΔT) between rocks within the channels and rocks halfway between the channels at the same depth. The relative temperature elevation near the channels is given by equation (A13) with $X = 1$

$$\Delta T = \left(\frac{-W_F \phi_C \rho_F C_{P,F}}{W_R \rho_R C_{P,R} + W_F \phi_C \rho_F C_{P,F} + W_F (1 - \phi_C) \rho_S C_{P,S}} \right) \left(\frac{v_F W_R^2 \rho_R C_{P,R}}{2K_R} \right) \left(\frac{\partial T}{\partial z} \right). \quad (14)$$

$2W_F v_F \phi_C$ is the total flux of fluid in a channel of porosity ϕ_C . W_F and W_R are the half-widths of the channel and rock slabs, respectively. For large values of W_R/W_F , (14) simplifies to

$$\Delta T = - \frac{v_F \phi_C W_F W_R \rho_F C_{P,F}}{2K_R} \left(\frac{\partial T}{\partial z} \right). \quad (15)$$

It is clear from (15) that the local thermal effect of fluid flowing in channels can be increased by increasing the fluid flux ($v_F \phi_C W_F$), increasing the separation (W_R) of the channels, and by increasing the temperature gradient ($\partial T/\partial z$) parallel to the channels.

ΔT calculated from equation (15) is shown on a logarithmic scale in Fig. 6 as a function of the logarithm of W_R for ($\partial T/\partial z$) of 0.03 K/m and various values of the fluid flux per unit length of channel $v_F \phi_C W_F$. For channel spacings (W_R) less than 1 km, fluxes approaching 10^{-7} (m^3 of fluid/ms) are needed to create steady state temperature differences (ΔT) greater than 10 K. Based on this result it appears that significant local deviations from the regional geotherm due to fluid flow in narrow channels are only possible for large volumes of fluid flow on widely separated channels.

One of the useful implications of equation (15) is that the distinction between pervasive flow of fluids and channelized flow of fluids is unimportant for *thermal* models of regional metamorphism, as long as the channels are not too isolated or the fluid flows unusually large. Results obtained using the simpler mathematics of pervasive flow can, therefore, be applied with confidence, even if detailed information about fluid pathways is unavailable.

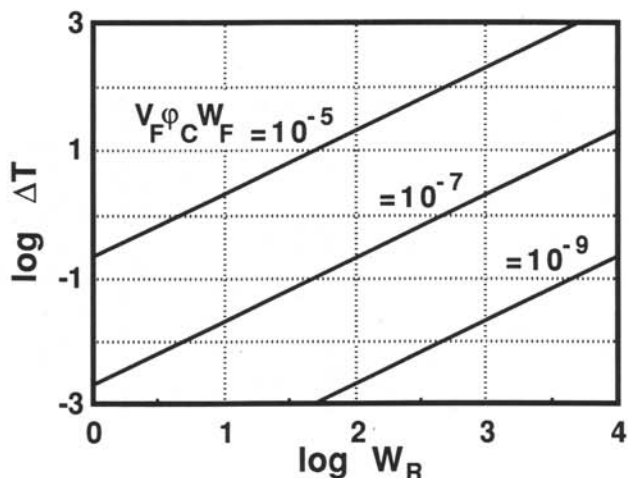


FIG. 6. The maximum steady state temperature difference ΔT (K) between the rocks in a fluid flow channel and the rocks halfway between the channels as predicted by equation (15) is shown on a logarithmic scale as a function of the logarithm of the half-distance between channels W_R (m) and the fluid flux per unit length of channel $v_F \phi_C W_F$ (m^3 fluid/ms).

Conversely, the *temperature* memory of metamorphic mineral assemblages is not likely to be of much assistance in elucidating the fine structure of volatile transport, such as the identification of metamorphic aquifers.

To obtain the convenience of the analytical solution (15), the assumption of a steady state and of an infinite system were used. Both of these assumptions warrant some examination. In particular, the finite thickness of the crust along with the constraint of constant temperature at the earth's surface are at odds with a picture of isotherms forever advancing upward. The limitations of these assumptions were removed and the success of equation (15) in estimating the maximum temperature rise in the vicinity of fluid flow channels was explored using two-dimensional finite difference calculations. Boundary conditions for the numerical models were: (1) constant temperature at the bottom and top of a rectangle of rock giving an initial linear temperature gradient; (2) a constant upward flux of fluid in a channel along one side of the rectangle; (3) vertical planes of symmetry (no heat flow) bounding the rectangular rock plus channel (as in Fig. 5), and (4) uniform temperature within the channel at any depth z .

Results of two numerical experiments simulating 10^6 a of fluid flow (near steady state) are shown in Figs 7 and 8. In both experiments, fluid fluxes of 3.6×10^{-8} (m^3 fluid/ m^2s) were directed upward along 20 m wide planar channels ($W_F = 10$ m) through a 10 km crust that initially sustained a 20 K/km gradient. In the experiment shown in Fig. 7A, the channels of fluid flow were separated by 20 km of rock ($W_R = 9990$ m). In Fig. 7B, the channels of fluid flow were separated by 2 km of rock ($W_R = 990$ m). In both Fig. 7A and 7B, final temperatures are contoured at 20 K intervals. When averaged over the horizontal distance shown, the volatile flux supplied in Fig. 7B is an order of magnitude larger than the volatile flux in Fig. 7A. Were this volatile flow pervasive, the parameter B defined in equation (4) would be 0.5 for Fig. 7A and 5.0 for Fig. 7B. The bunching of isotherms near the top of Fig. 7B follows closely that predicted for pervasive fluid flow with $B = 5.0$ in Fig. 1. Similarly, the isotherm spacing at the sides of Fig. 7A follows closely the prediction for $B = 0.5$ given in Fig. 1.

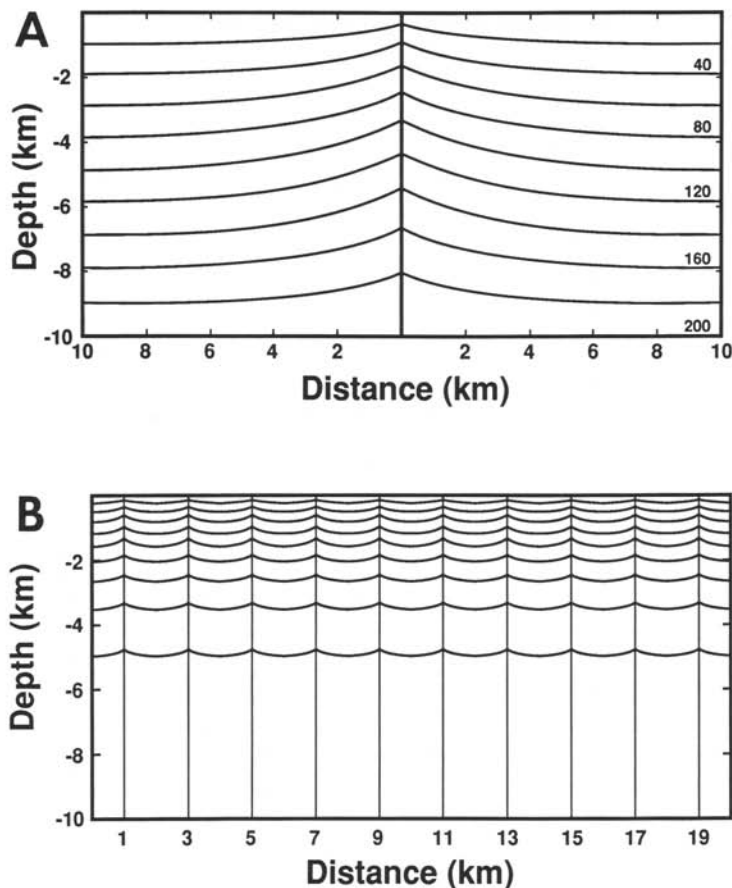


FIG. 7. Isothermal contours for the near steady state results of 1 Ma numerical simulations of channelized fluid flow are shown for (A) a channel spacing interval of 20 km and (B) a channel spacing interval of 2 km. In each case a volatile flux ($v_F \phi_C$) of 3.6×10^{-8} (m^3 fluid/ m^2 s) was directed upward along tabular vertical channels 20 m wide. Temperatures at the top and bottom of the 10 km rock slab were held constant at 0 and 200 K, respectively. The isotherm interval is 20 K.

Of particular interest is the difference in temperature (ΔT) between the rocks adjacent to the channels and the rocks halfway between the channels. How closely do the calculated ΔT s match those predicted by equation (15)? ΔT s for the experiments of Fig. 7A and 7B are shown in Fig. 8 as a function of depth along with the ΔT s predicted by equation (15). Although the ΔT predicted by equation (15) for the conditions of Fig. 7A is well above the 'observed' ΔT s, the ΔT predicted for the conditions of Fig. 7B is straddled by the 'observed' ΔT s. The underestimate by equation (15) of ΔT for the conditions of Fig. 7B may be attributed to the high temperature gradients near the surface of the earth that result when the averaged B is large. If the temperature gradients ($\partial T/\partial z$) calculated from the averaged B with equation (5) are used in equation (15), the predicted maximum ΔT s exceed the 'observed' ΔT 's in all cases.*

* Only ($\partial T/\partial z$) values from equation (5) that exceed the average (no fluid flow) ($\partial T/\partial z$) should be substituted for this average.

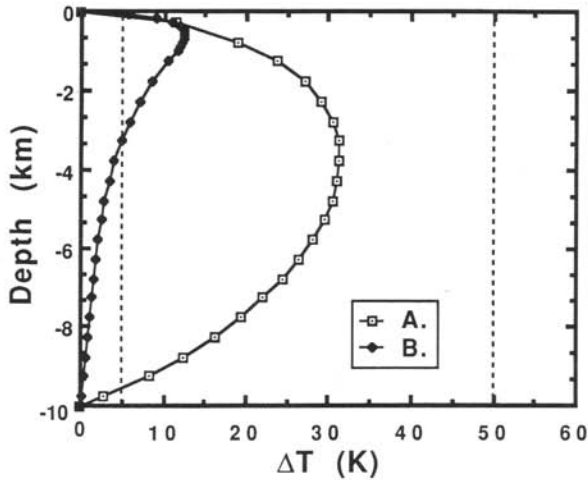


FIG. 8. The temperature difference ΔT (K) between the rocks in fluid flow channel and the rocks halfway between the channels is shown as a function of depth for the 1 Ma (near steady state) results of the numerical experiments of Figures 7A and 7B. These 'observed' temperature differences may be compared with the predictions of equation (15), shown as dotted vertical lines ($\Delta T=49.9$ and $\Delta T=49.5$, respectively), for the same fluid fluxes.

Overall, the numerical experiments confirm the predictions of the idealized solution (15): except for very large channel spacings ($W_R > 10$ km) and/or very large fluid fluxes per unit length of channel ($v_F \phi_C W_F > 10^{-8}$ m³ fluid/ms), the temperature of rocks near channels of fluid flow will not be more than a few degrees higher than the temperature of rocks halfway between the channels. Higher ΔT s are produced for regions with higher initial geothermal gradients. Equation (15) may underestimate the local temperature rise if the regional average flow gives a large value of B (equation 4).

Transient channelized flow

Continuing fluid flow until a steady state is achieved will produce the maximum absolute temperature increases relative to a conduction only steady state. However, large channelized fluid fluxes for short times can produce temporary local temperature differences that would not persist if the fluid flow continued. In other words, because of the finite thermal diffusivity of rocks, temperatures may rise more rapidly near channels of fluid flow than in the rocks halfway between the channels. Therefore, the ΔT between the rocks in the channels and the rocks halfway between the channels is maximized prior to the attainment of a steady state. If the mineral assemblages present can record the maximum temperatures achieved during a thermal transient produced by short-term channelized flow, thermobarometry may be able to identify the conduits for this transient flow.

Results of a two-dimensional numerical experiment involving fluid flow for 5000 a at 3.6×10^{-7} (m³ fluid/m²s) through planar channels distributed as in Fig. 7B ($B=50.0$) are shown in Fig. 9. Profiles of the temperature difference (ΔT) between the channel rocks and the rocks halfway between channels (at the same depth) are shown for $t=500$ a and $t=5000$ a. Although channel temperatures begin to fall immediately when the fluid flow stops at 5000 a, the temperatures of the rocks between the channels continue to rise. Therefore, the difference between the maximum temperature reached by the channels and the maximum temperature reached by the rocks halfway between the channels (shown at time 100 000 a in Fig. 9) is less than the ΔT for 5000 a.

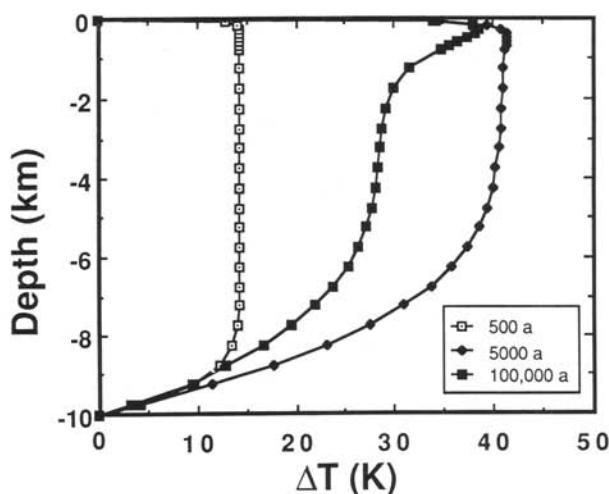


FIG. 9. The temperature difference ΔT (K) between the rocks in a fluid flow channel and the rocks halfway between the channels is shown as a function of depth for times $t = 500$ a and $t = 5000$ a during a numerical experiment in which a fluid flux of 3.6×10^{-7} (m^3 fluid/ m^2 s) was directed along channels with the geometry of those in Fig. 7B for a period of 5000 a. The maximum temperatures achieved by these same rocks within 100 000 a from the start of the transient were used to calculate the ΔT listed as $t = 100\,000$ a. By 100 000 a all rocks were cooling toward the conduction-only steady state.

Based on the data presented earlier in this paper, a volatile flux within the channels of 3.6×10^{-7} (m^3 fluid/ m^2 s) is not likely to persist for long in a metamorphic terrane. Nevertheless, a combination of special circumstances, such as a thermal excursion due to a magmatic intrusion combined with a fertile discontinuous devolatilization reaction in the adjacent country rocks, might produce very high volatile fluxes for short periods. If these high fluxes are channelized, their transient temperature effects may leave a permanent record in the rocks they traverse.

Wide channels

If the channels of volatile flow are too wide, the combination of fluid mixing and heat conduction within the channels may not maintain uniform temperatures across the channels, as assumed in the models described above. If this were the case, then temperatures would rise in the center of the channels relative to the sides, creating local temperature differences exceeding those predicted by equation (15). How wide must the channels be for this to be a concern? Once again, Carslaw & Jaeger (1959, eq. 2.11.9) have anticipated the problem and provide a useful solution. A channel of fluid flow may be treated as a zone of heat production with no heat production in the rock outside the channel. Their solution is for a semi-infinite system that should maximize the predicted effect, by analogy with the isolated and parallel channel models given above. For a channel of width $2W_F$, their solution is

$$T = \frac{A_0 W_F^2 \gamma}{4K_R} \left[1 - 2i^2 \operatorname{erfc} \left(\frac{1-X}{\sqrt{\gamma}} \right) - 2i^2 \operatorname{erfc} \left(\frac{1+X}{\sqrt{\gamma}} \right) \right] \quad 0 < X < 1 \quad (16)$$

$$T = \frac{A_0 W_F^2 \gamma}{4K_R} \left[2i^2 \operatorname{erfc} \left(\frac{X-1}{\sqrt{\gamma}} \right) - 2i^2 \operatorname{erfc} \left(\frac{X+1}{\sqrt{\gamma}} \right) \right] \quad X > 1 \quad (17)$$

where $i^2 \operatorname{erfc}$ is the second integral of the erfc error function (Carslaw & Jaeger, 1959, Appendix II), $X \equiv x/W_F$ is normalized distance measured from the channel center perpendicular to the channel, z is distance along the channel, and $\gamma \equiv 4\kappa t/W_F^2$ is a dimensionless parameter. The heat production due to fluid flow A_0 ($\text{J}/\text{m}^3\text{s}$) is given by

$$A_0 \equiv v_F \varphi_F \rho_F C_{P,F} \left(\frac{\partial T}{\partial z} \right), \quad (18)$$

and the other terms are as defined previously. In using this result, the thermal conductivities and heat capacities of the rock and channel are assumed to be identical.

Because all temperatures rise continuously in the vicinity of the channel for this model, equations (16) and (17) have been normalized for plotting by dividing the calculated temperatures by the temperature at the center of the channel. Figure 10 shows the temperatures calculated from equations (16)–(18) as a function of normalized distance X , measured from the center of the channel, for various values of the parameter γ . For $\gamma \geq 100$, it appears that little relative temperature gradient is expected across the channel. When fluid begins to flow in a channel, it is evident from Fig. 10 that there is an initial rise in temperature reflecting the fact that, initially, the temperature gradient is too low to cause the heat added to the channel to be conducted away as rapidly as it is added. The temperature gradient at the channel boundary rises with time (Fig. 11) so that at long times ($\gamma \geq 100$) virtually all of the heat added to the channel is conducted away. In other words, for large values of γ (long times or narrow channels), the assumption that the fluid flowing in a channel transfers all its thermal energy to the adjacent rock is valid. Even for long times, however, the temperature will increase from the edge toward the center of a channel. The total increase (normalized by the fluid flux and channel width) is given in Fig. 11 (read the scale on the right) as a function of γ . For wide channels and/or high fluid fluxes, temperature variation across the channel may be significant. For a fluid flux of 10^{-10} ($\text{m}^3 \text{ fluid}/\text{m}^2\text{s}$), a temperature gradient of $30 \text{ K}/\text{km}$, and a volumetric heat capacity of $(\rho_F C_{P,F}) = 3.5 \times 10^6$ ($\text{J}/\text{m}^3\text{K}$), we have $A_0 = 1.0 \times 10^{-5}$ ($\text{J}/\text{m}^3\text{s}$). For $W_F = 1000 \text{ m}$ and $\gamma = 100$, the temperature difference ΔT (K)

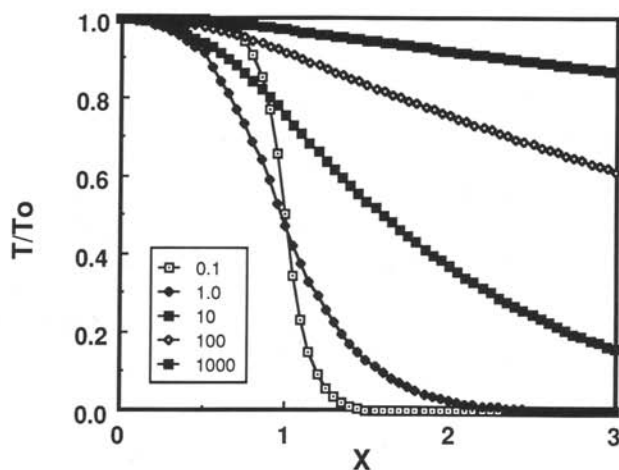


FIG. 10. Normalized temperature T/T_0 is shown as a function of normalized distance $X = x/W_F$ for various values (0.1, 1.0, 10, 100, 1000) of the dimensionless parameter $\gamma \equiv 4\kappa t/W_F^2$ for equation (2.11.9) of Carslaw & Jaeger (1959). The figure shows the evolution of the temperature profile across a $2W_F$ -meter-wide zone of heat production (= fluid flow) and into the surrounding rock. $X=0$ is a plane of symmetry.

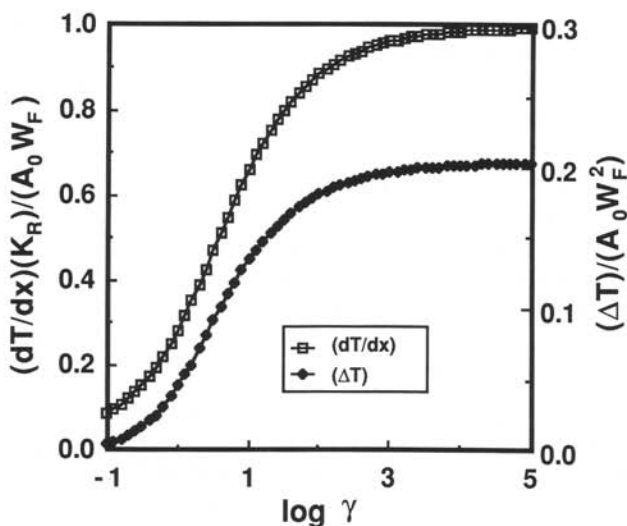


FIG. 11. The normalized heat flux across the boundary $(dT/dx)(K_R)/(A_0 W_F)$ and the normalized temperature elevation at the center relative to the boundary $(\Delta T)/(A_0 W_F^2)$ are shown for a model zone of heat production (= fluid flow) as a function of the logarithm of the dimensionless parameter $\gamma \equiv 4\kappa t/W_F^2$ as described by equation (2.11.9) of Carslaw & Jaeger (1959). The normalized heat flux (left scale) approaches 1.0 as the heat flux out of the zone approaches the heat produced within the zone for γ s exceeding 100. The temperature increase within the zone approaches $(0.2)(A_0 W_F^2)$, also for γ s exceeding 100.

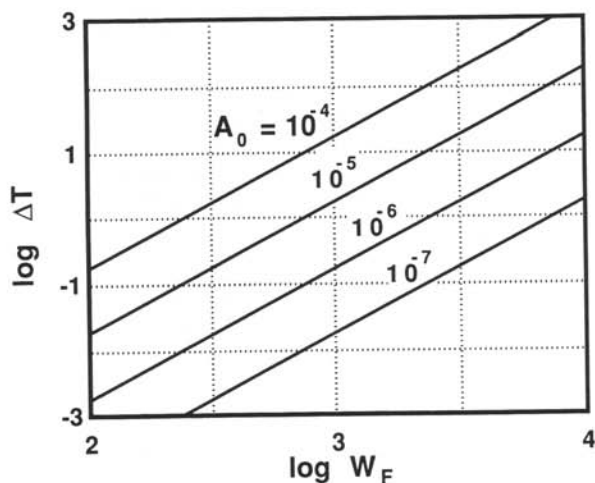


FIG. 12. The temperature difference ΔT (K) between the center ($X=0$) and edge ($X=1$) of a wide channel of fluid flow as given by equations (16) and (17) is shown on a logarithmic scale as a function of the logarithm of the channel half-width W_F (m) for $\gamma=100$ and various values of A_0 , the heat production due to fluid flow within the channel.

between the center and the edge of the channel is 1.78 K; for $W_F = 10\,000$ m, $\Delta T = 178$ K (see Fig. 12).

If the heat added to a channel by fluid flow is not balanced by heat loss to the surrounding rocks within 10^4 a, then it is not appropriate to apply the steady-state, parallel channel model (equation 15) to a fluid flow event lasting less than 1 Ma. For $\gamma=100$ and $t=10^4$ a, $2W_F = 200$ m would be a maximum channel width for which equation (15) might be used.

Evidently, channels wider than one km will retain a significant portion of the heat added by fluid flow, rather than losing this heat to the surroundings. For these wide zones of flow, a return to equation (6) will yield maximum temperature increases for the center of the channel relative to the surrounding rocks.

Chamberlain & Rumble (1988) describe 'metamorphic hot spots' in New Hampshire that are approximately 10 km^2 in area and spaced on roughly a 50 km grid. If all of the fluid in the 2500 km^2 area surrounding each metamorphic hot spot was focused into the hot spot, a focusing factor of 250 would apply. Taking a scale length L of 20 km, a temperature gradient of 30 K/km, $K_R = 2.5 \text{ (J/msK)}$, and $(\rho_F C_{P,F}) = 3.5 \times 10^6 \text{ (J/m}^3\text{K)}$, a fluid flux of $v_F \phi = 7.2 \times 10^{-11} \text{ (m}^3 \text{ of fluid/m}^2\text{s)}$ (a focusing factor of 4 over the probable maximum rate of fluid production) will yield $B = 2.0$ and within about 10^5 a Chamberlain & Rumble's observed temperature increase of about 100 K. Given the large possible focusing factor and the estimates given above for volatile production from pelites, a volatile-flow origin for Chamberlain & Rumble's metamorphic hot spot appears reasonable. Metamorphic hot spots like those described by Chamberlain & Rumble may provide the best *thermal* record of volatile flow in metamorphic terranes.

The Naxos thermal dome described by Schuiling & Kreulen (1979) and others extends over about a 250 km^2 area and records temperatures about 300 K higher in its center than in the region around it. If the dome was formed by a flux of CO_2 from the mantle as Schuiling & Kreulen suggest, a scale length of as much as 100 km might apply. Using $L = 10^5 \text{ m}$, a temperature gradient of 0.015 (K/m), $K_R = 2.5 \text{ (J/msK)}$, and $(\rho_F C_{P,F}) = 1.8 \times 10^6 \text{ (J/m}^3\text{K)}$, a CO_2 flux of about $3 \times 10^{-11} \text{ (m}^3 \text{ of fluid/m}^2\text{s)}$ giving $B = 2.0$ would produce the observed thermal dome in about 10^7 a. A larger fluid flux from a shallower depth would be necessary to produce the thermal dome in the less than the 10^7 a time interval that Schuiling & Kreulen conclude was available.

DISCUSSION

The major conclusion of this analysis is that single-pass volatile flow can be safely neglected in the thermal modeling of most metamorphic terranes. Whether the volatiles flow pervasively or in narrow channels, the regional thermal effect is the same. This conclusion is not due to any inherent thermal impotence on the part of flowing fluids, but rather to the absence of sufficient volumes of fluid to produce a significant temperature effect. If special circumstances lead to large volatile fluxes, such as the focusing of metamorphic or igneous volatiles into kilometer-scale zones, the temperature effects could be dramatic, if transient. Fortunately, mineral assemblages may record such thermal transients, so that careful field work may expose zones of volatile flow, if they occur. Peacock (1987a) reached similar conclusions in a numerical study of advection during metamorphism.

The kinds of structure, formation types, and tectonic regimes that might produce the necessary focusing of volatile flow can be imagined. For example, extensive fault zones are likely to play a role in volatile transport. It was noted above that the thermal effects of possible fluid flow in subduction zones have already been recognized (Davis *et al.*, 1986; Peacock, 1987b; Reck, 1987). However, Chamberlain & Rumble (1988) insist that their metamorphic hot spots cross-cut regional structures. They do observe a system of fractures of uncertain origin and suggest that the region may have been undergoing extension at the time of hot spot formation. Nevertheless, more observation is needed before the secrets of metamorphic plumbing are revealed. Fortunately, other measures of metamorphic fluid flow are more sensitive to the passage of volatiles than paleotemperatures recorded by mineral assemblages.

For geologists aware of geothermal systems and perhaps familiar with domestic hot water heat, the minimal thermal consequences of flowing metamorphic volatiles may seem counterintuitive, as it did to me. As is commonly the case, however, a simple calculation can improve one's intuition. If flowing fluids are to rival conduction in importance, they should transport an amount of heat that is comparable to the conductive heat flux. Using Fourier's law with $K_R = 2.5$ (J/mKs), a modest temperature gradient of 0.015 (K/m) will produce a conductive heat flux of 37.5 (mW/m²). For $\rho_F C_{p,F} = 3.5 \times 10^6$ (J/m³K), the extremely high fluid flux of 1.1×10^{-8} (m³ fluid/m²s) is needed to produce the same heat flux as conduction. The fact that a small fraction of this fluid flux can lead to thermal effects is a victory for intuition and justification for a more detailed analysis, but of limited consequence for thermal models of metamorphism.

ACKNOWLEDGEMENTS

I wish to thank Mike Albertson, Jim Callahan, and Robert Currier for mathematical tutoring, Nancy Agnew, Susan Melly, and Barbara Boothman for helping me tame various computers, Page Chamberlain for his advice and patience, and John Ashworth, Jack Cheney, Philip England, and Tom Hoisch for comments on the manuscript. Acknowledgement is made to the Donors of The Petroleum Research Fund, administered by the American Chemical Society, for partial support of this research.

REFERENCES

- Ahrens, T. J., & Schubert, G., 1975. Gabbro-eclogite reaction rate and its geophysical significance. *Rev. Geophys. Space Phys.* **12**, 383-400.
- Anderson, R. N., Delong, S. E., & Schwarz, W. M., 1978. Thermal model for subduction with dehydration in the downgoing slab. *J. Geol.* **86**, 731-39.
- 1980. Dehydration, asthenospheric convection and seismicity in subduction zones. *Ibid.* **88**, 445-51.
- Uyeda, S., & Miyashiro, A., 1976. Geophysical and geochemical constraints at converging plate boundaries, Part I: Dehydration in the downgoing slab. *Geophys. J. R. Astr. Soc.* **44**, 333-57.
- Beach, A., & Fyfe, W. S., 1972. Fluid transport and shear zones at Scourie, Sutherland: Evidence of overthrusting? *Contr. Miner. Petrol.* **36**, 175-80.
- Bebout, G. E., & Carlson, W. D., 1986. Fluid evolution and transport during metamorphism: Evidence from the Llano uplift, Texas. *Ibid.* **92**, 518-29.
- Bhattacharya, A., & Sen, S. K., 1986. Granulite metamorphism, fluid buffering, and dehydration melting in the Madras charnockites. *J. Petrology* **27**, 1119-42.
- Bickle, M. J., & McKenzie, D., 1987. The transport of heat and matter by fluids during metamorphism. *Contr. Miner. Petrol.* **95**, 384-92.
- Bottinga, Y., & Richet, P., 1981. High pressure and temperature equation of state and calculation of the thermodynamic properties of gaseous carbon dioxide. *Am. J. Sci.* **281**, 615-60.
- Brace, W. F., 1980. Permeability of crystalline and argillaceous rocks. *Int. J. Rock Mech. Min. Sci.* **17**, 241-51.
- 1984. Permeability of crystalline rocks: new in situ measurements. *J. geophys. Res.* **89**, 4327-30.
- Walsh, J. B., & Frangos, W. T., 1968. Permeability of granite under high pressure. *Ibid.* **73**, 2225-2236.
- Brady, J. B., 1975. Reference frames and diffusion coefficients. *Am. J. Sci.* **275**, 954-83.
- 1982. Thermal models of regional metamorphism. *Geol. Soc. Am. Abstr. Progr.* **14**, 451.
- Bredehoeft, J. D., & Papadopoulos, I. S., 1965. Rates of vertical groundwater movement estimated from the Earth's thermal profile. *Water Resour. Res.* **1**, 325-28.
- Burch, T. K., & Langseth, M., 1981. Heat-flow determinations in three DSDP boreholes near the Japan trench. *J. geophys. Res.* **86**, 9411-19.
- Burnham, C. W., 1979. Magmas and hydrothermal fluids. In: Barnes, H. L. (ed.) *Geochemistry of Hydrothermal Ore Deposits*, 2nd ed. New York: John Wiley, 71-136.
- Carlsaw, H. S., & Jaeger, J. C., 1959. *Conduction of Heat in Solids*. Oxford: Oxford University Press, 510 pp.
- Cathles, L. M., 1977. An analysis of the cooling of intrusives by ground-water convection which includes boiling. *Econ. Geol.* **72**, 804-26.
- Chamberlain, C. P., & England, P. C., 1985. The Acadian thermal history of the Merrimack synclinorium in New Hampshire. *J. Geol.* **93**, 593-602.

- Rumble, D., III. 1988. Thermal anomalies in a regional metamorphic terrain: An isotopic study of the role of fluids. *J. Petrology* **29**, 1215–32.
- Clark, S. P., & Jäger, E., 1969. Denudation rate in the Alps from geochronologic and heat flow data. *Am. J. Sci.* **267**, 1143–60.
- Cloos, M., 1984. Landward dipping reflectors in accretionary wedges: Active dewatering conduits? *Geology* **12**, 519–22.
- Crawford, M. L., & Hollister, L. S., 1986. Metamorphic fluids: The evidence from fluid inclusions. In: Walther, J. V., & Wood, B. J. (eds.) *Fluid–Rock Interactions During Metamorphism*. New York: Springer-Verlag, 1–35.
- Mark, L. E., 1982. Evidence from metamorphic rocks for overthrusting, Pennsylvania Piedmont, U.S.A. *Can. Miner.* **20**, 330–47.
- Criss, R. E., & Taylor, H. P., Jr., 1987. Meteoric-hydrothermal systems. In: Valley, J. W., Taylor, H. P., Jr., & O'Neil, J. R. (eds.) *Stable Isotopes in High Temperature Processes*. Washington, D.C.: Mineralogical Society of America, *Reviews in Mineralogy*, **16**, 373–424.
- Davis, D. M., Langseth, M., & Westbrook, G. K. 1986. Some hydrogeologic issues in accretionary prisms. *EOS Trans. Am. geophys. Union* **67**, 242.
- Davy, P., & Gillet, P., 1986. The stacking of thrust slices in collision zones and its thermal consequences. *Tectonics* **5**, 913–29.
- Delany, J. M., & Helgeson, H. C., 1978. Calculation of the thermodynamic consequences of dehydration in subducting oceanic crust to 100 kb and >800°C. *Am. J. Sci.* **278**, 638–86.
- Donaldson, I. G., 1962. Temperature gradients in the upper layers of the earth's crust due to convective water flows. *J. geophys. Res.* **67**, 3449–59.
- England, P. C., 1978. Some thermal considerations of the Alpine metamorphism, past, present, and future. *Tectonophysics* **46**, 21–40.
- Thompson, A. B., 1984. Pressure-temperature-time paths of regional metamorphism, I. Heat transfer during the evolution of regions of thickened continental crust. *J. Petrology* **25**, 894–928.
- Etheridge, M. A., Wall, V. J., & Vernon, R. H., 1983. The role of the fluid phase during regional metamorphism and deformation. *J. metamorphic Geol.* **1**, 205–26.
- Ferry, J. M., 1979. A map of chemical potential differences within an outcrop. *Am. Mineral.* **64**, 966–85.
- 1980. A case study of the amount and distribution of heat and fluid during metamorphism. *Contr. Miner. Petrol.* **71**, 373–85.
- 1983. Regional metamorphism of the Vassalboro Formation, south-central Maine, USA: a case study of the role of fluid in metamorphic petrogenesis. *J. geol. Soc. Lond.* **140**, 551–76.
- 1986a. Reaction progress: a monitor of fluid-rock interaction during metamorphic and hydrothermal events. In: Walther, J. V., & Wood, B. J. (eds.) *Fluid–Rock Interactions During Metamorphism*. New York: Springer-Verlag, 60–88.
- 1986b. Infiltration of aqueous fluid and high fluid-rock ratios during greenschist facies metamorphism: A reply. *J. Petrology* **27**, 695–714.
- 1987. Metamorphic hydrology at 13-km depth and 400–500°C. *Am. Miner.* **72**, 39–58.
- Fetter, C. W., Jr., 1980. *Applied Hydrogeology*. Columbus: Charles E. Merrill, 488 pp.
- Fowler, C. M. R., & Nisbet, E. G., 1982. The thermal background to metamorphism, II. Simple two-dimensional conductive models. *Geosci. Can.* **9**, 208–14.
- Fyfe, W. S., Price, N. J., & Thompson, A. B., 1978. *Fluids in the Earth's Crust*. Amsterdam: Elsevier, 383 pp.
- Griggs, D. T., 1972. The sinking lithosphere and the focal mechanism of deep earthquakes. In: Robertson, E. C., Hays, J. F., & Knopoff, L. (eds.) *The Nature of the Solid Earth*. New York: McGraw-Hill, 361–84.
- Hansen, E. C., Newton, R. C., & Janardhan, A. S., 1984. Fluid inclusions in rocks from the amphibolite-facies gneiss to charnockite progression in southern Karnataka, India: Direct evidence concerning the fluids of granulite facies metamorphism. *J. metamorphic Geol.* **2**, 249–64.
- Hasebe, R., Fujii, N., & Uyeda, S., 1970. Thermal processes under island arcs. *Tectonophysics* **10**, 335–55.
- Helgeson, H. C., & Kirkham, D. H., 1974. Theoretical prediction of the thermodynamic behavior of aqueous electrolytes at high pressures and temperatures. I. Summary of the thermodynamic/electrostatic properties of the solvent. *Am. J. Sci.* **274**, 1089–1198.
- Hoisch, T. D., 1987. Heat transport by fluids during Late Cretaceous regional metamorphism in the Big Maria Mountains, southeastern California. *Geol. Soc. Am. Bull.* **98**, 549–53.
- Hollister, L. S., 1982. Metamorphic evidence for rapid (2 mm/yr) uplift of a portion of the central gneiss complex, Coast Mountains, B.C. *Can. Miner.* **20**, 319–32.
- Honda, S., 1985. Thermal structure beneath Tohoku, northeast Japan—A case study for understanding the detailed thermal structure of the subduction zone. *Tectonophysics* **112**, 69–102.
- Uyeda, S., 1983. Thermal processes in subduction zones—A review and preliminary approach on the origin of arc volcanism. In: Shimozuru, D., & Yokoyama, I., (eds.) *Arc Volcanism—Physica and Tectonics. Adv. Earth Planet. Sci.* 117–40.
- Hubbert, M. K., 1940. The theory of ground-water motion. *J. Geol.* **48**, 785–944.
- Jaeger, J. C., 1964. Thermal effects of intrusions. *Rev. Geophys.* **2**, 443–66.
- Jaupart, C., & Provost, A., 1985. Heat focussing, granite genesis and inverted metamorphic gradients in continental collision zones. *Earth planet. Sci. Lett.* **73**, 385–97.

- Kerrick, R., La Tour, T. E., & Willmore, L., 1984. Fluid participation in deep fault zones: Evidence from geological, geochemical, and $^{18}\text{O}/^{16}\text{O}$ relations. *J. geophys. Res.* **89**, 4331–43.
- McKenzie, D. P., 1969. Speculations on the consequence and causes of plate motions. *Geophys. J. R. Astr. Soc.* **18**, 1–32.
- 1978. Some remarks on the development of sedimentary basins. *Earth planet Sci. Lett.* **40**, 25–32.
- 1981. The variation of temperature with time and hydrocarbon maturation in sedimentary basins formed by extension. *Ibid.* **55**, 87–98.
- Nabelek, P. I., Labotka, T. C., O'Neil, J. R., & Papike, J. J., 1984. Contrasting fluid/rock interaction between the Notch Peak granitic intrusion and argillites and limestones in western Utah: Evidence from stable isotopes and phase assemblages. *Contr. Miner. Petrol.* **86**, 25–34.
- Newton, R. C., 1986. Fluids of granulite facies metamorphism. In: Walther, J. V., & Wood, B. J. (eds.) *Fluid–Rock Interactions During Metamorphism*. New York: Springer-Verlag, 36–59.
- Nisbet, E. G., & Fowler, C. M. R., 1982. The thermal background to metamorphism, I. Simple one-dimensional conductive models. *Geosci. Can.* **9**, 161–4.
- Norris, R. J., & Henley, R. W., 1976. Dewatering of a metamorphic pile. *Geology* **4**, 333–6.
- Norton, D., & Knight, J., 1977. Transport phenomena in hydrothermal systems: cooling plutons. *Am. J. Sci.* **277**, 937–81.
- Oxburgh, E. R., & Turcotte, D. L., 1970. The thermal structure of island arcs. *Geol. Soc. Am. Bull.*, **81**, 1665–88.
- 1971. Origin of paired metamorphic belts and crustal dilation in island arc regions. *J. geophys. Res.* **76**, 1315–27.
- 1974. Thermal gradients and regional gradients in overthrust terrains with special reference to the Eastern Alps. *Schweiz. miner. petrogr. Mitt.* **54**, 641–62.
- 1976. The physico-chemical behavior of the descending lithosphere. *Tectonophysics* **32**, 107–28.
- Peacock, S. M., 1986. Rates of contact and regional metamorphism. *Geol. Soc. Am. Abstr. Progr.* **18**, 715.
- 1987a. Advective heat transfer by metamorphic fluid flow. *EOS Trans. Am. geophys. Union* **68**, 466.
- 1987b. Thermal effects of metamorphic fluids in subduction zones. *Geology* **15**, 1057–1060.
- Pratt, H. R., Swolfs, H. S., & Lingle, R., 1977. In situ and laboratory measurements of velocity and permeability. In: Heacock, J. G. et al. (ed.) *The Earth's Crust: Its Nature and Physical Properties*. Am. geophys. Union geophys. Monogr. **20**, 215–31.
- Reck, B. A., 1987. Implications of measured thermal gradients for water movement through the northeast Japan accretionary prism. *J. geophys. Res.* **92**, 3683–90.
- Richardson, S. W., 1970. The relation between a petrogenetic grid, facies series, and the geothermal gradient in metamorphism. *Fortschr. Miner.* **47**, 65–76.
- Powell, R., 1976. Thermal causes of the Dalradian metamorphism in the central highlands of Scotland. *Scott. J. Geol.* **12**, 237–68.
- Royden, L. H., & Hodges, K. V., 1984. A technique for analyzing the thermal and uplift histories of eroding orogenic belts: a Scandinavian example. *J. geophys. Res.* **89**, 7091–106.
- Keen, C. E., 1980. Rifting process and the thermal evolution of the continental margin of eastern Canada determined from subsidence curves. *Earth planet. Sci. Lett.* **51**, 343–61.
- Rubie, D. C., 1984. A thermal-tectonic model for high-pressure metamorphism and deformation in the Sesia zone, Western Alps. *J. Geol.* **92**, 21–36.
- Rumble, D., III, Ferry, J. M., Hoering, T. C., & Boucot, A. S., 1982. Fluid flow during metamorphism of the Beaver Brook fossil locality, New Hampshire. *Am. J. Sci.* **282**, 886–919.
- Spear, F. S., 1983. Oxygen-isotope equilibration and permeability enhancement during regional metamorphism. *J. geol. Soc. Lond.* **140**, 619–28.
- Rye, R. O., Schuiling, R. D., Rye, D. M., & Jansen, J. B. H., 1976. Carbon, hydrogen, and oxygen isotope studies of the regional metamorphic complex at Naxos, Greece. *Geochim. cosmochim. Acta* **40**, 1031–49.
- Sandiford, M., & Powell, R., 1986. Deep crustal metamorphism during continental extension: modern and ancient examples. *Earth planet. Sci. Lett.* **79**, 151–8.
- Schuiling, R. D., & Kreulen, R., 1979. Are thermal domes heated by CO_2 -rich fluids from the mantle. *Ibid.* **43**, 298–302.
- Sharp, J. M., Jr., & Domenico, P. A., 1976. Energy transport in thick sequences of compacting sediment. *Geol. Soc. Am. Bull.* **87**, 390–400.
- Shimazu, Y., 1961. A geophysical study of regional metamorphism. *Japan J. Geophys.* **2**, 135–76.
- Skempton, A. W., 1970. The consolidation of clays by gravitational compaction. *Geol. Soc. Lond. Q. J.*, **125**, 373–411.
- Spera, F. J., 1981. Carbon dioxide in igneous petrogenesis: II. Fluid dynamics of mantle metasomatism. *Contr. Miner. Petrol.* **77**, 56–65.
- Stallman, R. W., 1963. Computation of ground-water velocity from temperature data. In: Bentall, R. (ed.) *Methods of Collecting and Interpreting Ground-Water Data*. U.S. Geol. Survey Water Supply Pap., 1544-H, 36–46.
- Stegena, L., 1982. Water migration influences on the geothermics of basins. *Tectonophysics*, **83**, 91–99.
- Sydora, L. J., Jones, F. W., & Lambert, R. St. J., 1978. The thermal regime of the descending lithosphere: The effect of varying angle and rate of subduction. *Can. J. Earth Sci.* **15**, 626–41.
- Taylor, H. P., Jr., 1971. Oxygen isotope evidence for large-scale interaction between meteoric ground waters and

- Tertiary granodiorite intrusions, Western Cascade Range, Oregon. *J. geophys. Res.* **76**, 7855–74.
- Toksöz, M. N., Minear, J. W., & Julian, B. R., 1971. Temperature field and geophysical effects of a downgoing slab. *Ibid.* **76**, 1113–38.
- Walther, J. V., & Orville, P. M., 1982. Volatile production and transport in regional metamorphism. *Contr. Miner. Petrol.* **79**, 252–57.
- Walton, M., 1960. Molecular diffusion rates in supercritical water vapor estimated from viscosity data. *Ann. J. Sci.* **258**, 385–401.
- Wang, C.-Y., & Shi, Y.-L., 1984. On the thermal structure of subduction complexes: A preliminary study. *J. geophys. Res.* **89**, 7709–18.
- Wells, P. R. A., 1980. Thermal models for the magmatic accretion and subsequent metamorphism of continental crust. *Earth planet Sci. Lett.* **46**, 253–65.
- Wickham, S. M., & Oxburgh, E. R., 1985. Continental rifts as a setting for regional metamorphism. *Nature* **318**, 330–33.
- Taylor, H. P., Jr., 1985. Stable isotopic evidence for large-scale seawater infiltration in a regional metamorphic terrane; the Trois Seigneurs Massif, Pyrenees, France. *Contr. Miner. Petrol.* **91**, 122–37.
- Wood, B. J., & Walther, J. V., 1986. Fluid flow during metamorphism and its implications for fluid-rock ratios. In: Walther, J. V., & Wood, B. J., (eds.) *Fluid–Rock Interactions During Metamorphism*. New York: Springer-Verlag, 89–108.
- Yardley, B. W. D., 1986. Fluid migration and veining in the Connemara schists, Ireland. *Ibid.* 109–31.

APPENDIX: STEADY CHANNELIZED FLUID FLOW IN AN INFINITE SLAB

One route to a solution involving channelized flow is to neglect all fluid flow other than that in the channels, dividing the crust into regions of heat transfer by conduction *and* fluid flow (the channels) and regions of heat transfer by conduction only (the rock). The solution is simplified if these regions are parallel slabs of infinite extent distributed symmetrically with respect to one another (Figure 5). Specifically, with this geometry the problem is reduced to two dimensions ($\delta T/\delta y = 0$ for all y) and there is no heat flow across the planes of symmetry ($\delta T/\delta x = 0$ at the mirror planes). Let there be fluid only in the channels (to simplify the equations) and let the fluid in the channels be well-stirred perpendicular to the slab so that T is constant for all x and y at any z within the channels. Let there be an initial constant temperature gradient ($\delta T/\delta z = g_z$) within both the channels and the rock. If the fluid begins to flow at a constant rate in the z direction, a steady state will be established eventually with curved isotherms bending ‘downstream’ near the channels (Fig. 5) and moving at a constant velocity (much slower than the fluid). The shape of these isotherms is constant and describes the expected relative temperature rise in the vicinity of a tabular fluid channel through which a fluid is flowing.

Consider the energy flux into the space bounded by an infinitesimal cube in the rock that moves at the same velocity as the isotherms in the z direction. Relative to this cube (the isotherm reference frame, IRF), temperatures and the shape of the isotherms do not change ($\delta T/\delta t = 0$). Therefore, the net energy flux into this cube must be zero. The net energy gain or loss E_x in the cube by conduction across its yz faces is given by (Carslaw & Jaeger, 1959, p. 8):

$$E_x = - \left(\frac{\partial J_x}{\partial x} \right) = K_R \left(\frac{\partial^2 T}{\partial x^2} \right) \quad (\text{A1})$$

where J_x is the heat flux ($\text{J/m}^2\text{s}$) in the x direction and K_R is the thermal conductivity (J/msK) of the rock. The net energy gain or loss E_y by conduction across the xz faces is zero because $\delta T/\delta y = 0$. The heat flux in the z direction *relative to the moving cube* J_z^{IRF} is (compare Brady, 1975):

$$J_z^{\text{IRF}} = J_z^{\text{fixed}} - v_z^{\text{IRF}} (\rho_R C_{P,R} T) \quad (\text{A2})$$

where J_z^{fixed} is the heat flux in the z direction with respect to a fixed reference frame, v_z^{IRF} is the velocity of the isotherm reference frame (and cube) with respect to a fixed reference frame, ρ_R is the density and $C_{P,R}$ the specific heat capacity of the rock. Using (A2), the net energy flux across the xy faces E_z is found to be

$$E_z = - \left(\frac{\partial J_z^{\text{IRF}}}{\partial z} \right) = v_z^{\text{IRF}} \rho_R C_{P,R} \left(\frac{\partial T}{\partial z} \right) \quad (\text{A3})$$

because the temperature gradient is linear in the z direction ($\delta^2 T/\delta z^2 = 0$). Now

$$\left(\frac{\partial T}{\partial t} \right)^{\text{IRF}} \equiv 0 = \frac{E_x + E_y + E_z}{\rho_R C_{P,R}} = \frac{K_R}{\rho_R C_{P,R}} \left(\frac{\partial^2 T}{\partial x^2} \right) + v_z^{\text{IRF}} \left(\frac{\partial T}{\partial z} \right). \quad (\text{A4})$$

Substituting the dimensionless parameter $X \equiv x/W_R$ for x , where W_R is the half width of the rock between channels as identified in Fig. 5, Equation (A4) may be rearranged to yield

$$\left(\frac{\partial^2 T}{\partial X^2}\right) = -\frac{W_R^2 v_z^{\text{IRF}} \rho_R C_{P,R}}{K_R} \left(\frac{\partial T}{\partial z}\right) = k_1 \quad (\text{A5})$$

where k_1 is a constant.

The solution to (A5) is of the form

$$T = AX^2 + BX + C. \quad (\text{A6})$$

If $T = T_0$ at $X = 0$, then $C = T_0$. Also at $X = 0$, $(\partial T/\partial X) = 0$ because of the symmetry plane there, so $B = 0$. And recalling (A5), it is clear that $2A = k_1$. Thus,

$$T - T_0 = \frac{k_1}{2} X^2 = -\frac{W_R^2 v_z^{\text{IRF}} \rho_R C_{P,R}}{2K_R} \left(\frac{\partial T}{\partial z}\right) X^2. \quad (\text{A7})$$

The velocity of the isotherm reference frame may be related to the velocity of the fluid in the channels as follows. In the isotherm reference frame at $X = 1$, the boundary of the fluid channels, the heat flux into the rock (per unit area) from the channel must equal the net energy gain in the channel (per unit volume) by conduction and fluid flow in the z direction. Using a modification of (A2) for the channels

$$J_z^{\text{IRF}} = J_z^{\text{fixed}} - v_z^{\text{IRF}} T [\varphi_C \rho_F C_{P,F} + (1 - \varphi_C) \rho_S C_{P,S}] \quad (\text{A8})$$

$$J_z^{\text{IRF}} = -K_F \left(\frac{\partial T}{\partial z}\right) + v_z^{\text{fluid}} \varphi_C \rho_F C_{P,F} T - v_z^{\text{IRF}} T [\varphi_C \rho_F C_{P,F} + (1 - \varphi_C) \rho_S C_{P,S}] \quad (\text{A9})$$

where K_F is the thermal conductivity, v_z^{fluid} is the velocity, ρ_F is the density and $C_{P,F}$ is the heat capacity of the fluid. φ_C is the connected porosity in the channels. ρ_S and $C_{P,S}$ are the density and specific heat of the solids in the channels. Because $(\partial T/\partial z)$ is constant, the net energy gain in a channel (per unit volume) with respect to the isotherm reference frame due to conduction and flow in the z direction is

$$-\left(\frac{\partial J_z^{\text{IRF}}}{\partial z}\right) = [v_z^{\text{fluid}} \varphi_C \rho_F C_{P,F} - v_z^{\text{IRF}} [\varphi_C \rho_F C_{P,F} + (1 - \varphi_C) \rho_S C_{P,S}]] \left(\frac{\partial T}{\partial z}\right). \quad (\text{A10})$$

Setting W_F times equation (A10) equal to the flux across one channel boundary to maintain the required constant temperature we have

$$\frac{K_R}{W_R} \left(\frac{\partial T}{\partial X}\right)_{X=1} = W_F [v_z^{\text{fluid}} \varphi_C \rho_F C_{P,F} - v_z^{\text{IRF}} [\varphi_C \rho_F C_{P,F} + (1 - \varphi_C) \rho_S C_{P,S}]] \left(\frac{\partial T}{\partial z}\right). \quad (\text{A11})$$

Substituting the first derivative of (A7) with respect to X for $(\partial T/\partial X)$, the left side of (A11) becomes

$$\frac{K_R}{W_R} \left(\frac{W_R^2 v_z^{\text{IRF}} \rho_R C_{P,R}}{K_R}\right) \left(\frac{\partial T}{\partial z}\right)$$

and (A11) may be rearranged to solve for v_z^{IRF} . The solution

$$v_z^{\text{IRF}} = v_z^{\text{fluid}} \left[\frac{W_F \varphi_C \rho_F C_{P,F}}{W_R \rho_R C_{P,R} + W_F \varphi_C \rho_F C_{P,F} + W_F (1 - \varphi_C) \rho_S C_{P,S}} \right] \quad (\text{A12})$$

may be inserted into (A7) to yield

$$T - T_0 = AX^2 \quad (\text{A13})$$

where

$$A = -v_z^{\text{fluid}} \left[\frac{W_F \varphi_C \rho_F C_{P,F}}{W_R \rho_R C_{P,R} + W_F \varphi_C \rho_F C_{P,F} + W_F (1 - \varphi_C) \rho_S C_{P,S}} \right] \left(\frac{W_R^2 \rho_R C_{P,R}}{2K_R}\right) \left(\frac{\partial T}{\partial z}\right).$$